Stem Cell Reports, Volume *11*

Supplemental Information

HOPX Defines Heterogeneity of Postnatal Subventricular Zone Neural Stem Cells

Stefan Zweifel, Guillaume Marcy, Quentin Lo Guidice, Deqiang Li, Christophe Heinrich, Kasum Azim, and Olivier Raineteau

Inventory of Supplemental Information

1) Supplementary experimental procedures
2) references related to experimental procedures
3) Supplementary figures S1 to S6 with legends

1) Supplementary Experimental Procedures

Plasmids

The following plasmids were used in this study: pCX-GFP (kind gift of X Morin, ENS, Paris; France); pFloxpA-DsRed express (kind gift of Colette Dehay; INSERM U1208, Bron, France); pCAG-Cre (Addgene; 13775); pCMV-Hopx (Open Biosystems; MMM1013-202767606); pPB-CAG-EmGFP (VB161220-1119syh; VectorBuilder Inc., Cyagen Bioscience, Santa Clara, California, USA); pCMV-hyPBase (kind gift of Laura López-Mascaraque; Instituto Cajal, Madrid, Spain). Plasmids were purified using the EndoFree Plasmid Kit according to the manufacturer's protocol (Qiagen; 12362). Plasmids were re-suspended to a final concentration of 5 µg/µl. Dorsal electroporations were performed in P1 to P2 (postnatal day 1 to 2) pups as previously described (Fernández et al., 2011). In $Hopx^{CreERT2}$ animals subcutaneous tamoxifen (Tam; SIGMA-Aldrich; T5648) administration (1 mg per pup) was performed 2 to 3 hrs after electroporation.

Primary Antibodies for Immunohistochemistry

The following primary antibodies were used for immunohistochemical procedures: Rabbit anti-Hopx (1:400; Santa Cruz; sc-30216); Mouse anti-Hopx (1:400; Santa Cruz; sc-398703); Goat anti-DCX (1:500; Santa Cruz; sc-8066); Mouse anti-Olig2 (1:1500; Millipore; MABN50); Mouse anti-GFAP (1:500; Millipore; MAB3402); Chicken anti-GFP (1:1000; AVES LABS; GFP-1020); Rabbit anti-RFP (1:1500; MBL; PM005); Rabbit anti-S100β (1:5000; SWANT); Chicken anti-βGal (1:4000; Abcam; ab9361); Goat anti-Mcm2 (1:300; Santa Cruz; sc-9839); Mouse anti-Sox2 (1:100; Santa Cruz; sc-365823); Rabbit anti-Blbp (1:300; Millipore; ABN14). Blocking was done in TNB buffer (0.1 M PB; 0.05% Casein; 0.25% Bovine Serum Albumin; 0.25% TopBlock) with 0.4% triton-X (TNB-Tx). Sections were incubated over night at 4°C with gentle shaking the following primary antibodies in TNB-Tx. Following extensive washing in 0.1 M PB with 0.4% triton-X (PB-Tx), sections were incubated with appropriate secondary antibodies conjugated with Alexafluor 488, 555 or 647 (1:500; Life Technologies) for 2 hrs at room temperature. Sections were washed and counterstained with Dapi (1:5000; Life Technologies; D1306). To increase the signal from YFP and βGal, biotinylated secondary antibodies (1:500; Jackson) were used in combination with DTAF conjugated streptavidin (1:250; Jackson) or a TSA amplification kit according to manufacturer's protocol (Life Technologies; T-20932), respectively.

FACsorting and qPCR

Hes5::EGFP (with C57BL/6 background) of the age P2-P4 were used for sorting for NSCs as previously described and using the exact same parameters (Azim et al. 2015). 4 to 5 animals of one litter was used for 1 "n" number. Microdissection of SVZ domains (dorso-medial; dorso-lateral and lateral) was performed in RNase free, sterile conditions. Microdissection of SVZ domains (dorso-medial; dorso-lateral and lateral) was performed in RNase free, sterile conditions. Tissues were dissociated using a trypsin-based Neural

Dissociation Kit (Miltenyi Biotec, Bergisch Gladbach, Germany). For additional purification of the Hes5-EGFP population, an APC conjugated NSC antibody against the transmembrane-protein prominin-1 (1:100; ebiosciences) was applied for 15 mins at RT, before suspension was subjected to Fluorescence Activated Cell Sorting (FACS Aria III; BD Bioscience, Franklin Lakes, New Jersey, USA). Dead cells were excluded by forward and sideward scatter. Gating settings were gained using an EGFP- wildtype animal and a prominin-1 isotype control conjugated to APC (rat anti-IgG; 1:100, ebiosciences). Brightest 30% of $EGFP^+$ cells, which where prominin-1^+ were collected directly into RNA lysis buffer and snap-frozen for further gene expression analysis. RNA extraction was performed using the RNeasy microkit (Qiagen; 74004) following manufacturer's guidelines. RNA amplification of 3 ng input material was done using the Nugene Pico Ovation WT kit (NuGen Technologies, Inc., San Carlos, CA) as described previously (Azim et al. 2015). qPCR was performed according to the procedures described elsewhere (Azim et al., 2012b, Azim et al., 2014b), with the LightCycler 480 (Roche, Basel, Switzerland). All reactions were performed in duplicates or triplicates and GAPDH was used as reference gene. Primers used were custom made by Qiagen (EGFP, Eomes, Hopx, Pcna, Sp8) or designed with the Primer Express 1.5 software and produced by Eurofins (Schönenwerd, Switzerland):

GAPDH:	fw_CGTCCCGTAGACAAAATGGT,	rv_TTGATGGCAACAATCTCCAC;
Aldh1l1:	fw_CAGTAAACCTCCTGGCCAAA,	rv_CCCTGTTTTCCCTACTTCCC;
Aqp4:	fw_TGAGCTCCACATCAGGACAG,	rv_TCCAGCTCGATCTTTTGGAC;
Dct:	fw_GCATCTGTGGAAGGGTTGTT,	rv_ACTCCTTCCTGAATGGGACC;
DCX:	fw_CTGACTCAGGTAACGACCAAGAC,	rv_TTCCAGGGCTTGTGGGTGTAGA;
Dlx2:	fw_CTTCTTGAACTTGGATCGGC,	rv_AGACCCAGTATCTGGCCCTG;
Ebf1:	fw_GGTGGAAGTCACACTGTCGTAC,	rv_GTAACCTCTGGAAGCCGTAGTC;
Fgfr3:	fw_ACAGGTGGTCATGGCAGAAGCT,	rv_CTCCATCTCAGATACCAGGTCC;
Gli1:	fw_CTCAAACTGCCCAGCTTAACCC,	rv_TGCGGCTGACTGTGTAAGCAGA;
Gli3:	fw_CGAGAACAGATGTCAGCGAG,	rv_TGAGGCTGCATAGTGATTGC;
Hes5:	fw_GTAGTCCTGGTGCAGGCTCT,	rv_AACTCCAAGCTGGAGAAGGC;
Id3:	fw_GCGTGTCATAGACTACATCCTCG,	rv_GTCCTTGGAGATCACAAGTTCCG;
Lef1:	fw_CGTCACACATCCCGTCAGATGTC,	rv_TGGGTGGGGTGATCTGTCCAACG;
Olig1:	fw_AGCAAGCTCAAACGTTGGTT,	rv_GTTCTGTTTTTCAGGCTCGC;
Olig2:	fw_GACGATGGGCGACTAGACA,	rv_CAGCGAGCACCTCAAATCTA;
PDGFRα:	fw_AGAAAATCCGATACCCGGAG,	rv_AGAGGAGGAGCTTGAGGGAG;
Plp1:	fw_GGGCCCCTACCAGACATCTA,	rv_TCCTTCCAGCTGAGCAAAGT;
Tcf7:	fw_TGCCTTCAATCTGCTCATGCC,	rv_GTGTGGACTGCTGAAATGTTCG;
Vax1:	fw_CTCTACAGGCTGGAGATGGAGT,	rv_GCTTAGTCCGCCGATTCTGGAA.

Meta-analysis of Transcriptional Profiles

To generate the lists of TFs that are enriched in dNSCs and lNSCs, we made use of our recently published transcriptional datasets (Azim et al., 2015; GSE60905). We analyzed the dataset on the "Gene Expression Omnibus" (https://www.ncbi.nlm.nih.gov/geo/) for transcripts that are differentially expressed between dNSCs and lNSCs (≥1.8 fold enrichment and p-values <5%). Finally, we selected transcripts for transcription factor activity and regulation of transcription using "DAVID Analysis Wizard" (https://david.ncifcrf.gov/). Lists of

transcripts were analyzed for enrichments in the neuronal, astrocytic or oligodendrocytic lineage using the transcriptional dataset of the Barres group (Cahoy et al., 2008; GSE9566). Heatmaps were produced using a self-made R script “Heatmap Generator”, which enables us to compare and generate heatmaps from different datasets available via the “Gene Expression Omnibus” (GEO).

2) REFERENCES

Azim, K., Raineteau, O., and Butt, A.M. (2012). Intraventricular injection of FGF-2 promotes generation of oligodendrocyte-lineage cells in the postnatal and adult forebrain. Glia *60*, 1977–1990.

Azim, K., Fischer, B., Hurtado-Chong, A., Draganova, K., Cantù, C., Zemke, M., Sommer, L., Butt, A., and Raineteau, O. (2014). Persistent Wnt / b -Catenin Signaling Determines Dorsalization of the Postnatal Subventricular Zone and Neural Stem Cell Specification into Oligodendrocytes and Glutamatergic Neurons. Stem Cells *23*, 1301–1312.

Azim, K., Hurtado-Chong, A., Fischer, B., Kumar, N., Zweifel, S., Taylor, V., and Raineteau, O. (2015). Transcriptional Hallmarks of Heterogeneous Neural Stem Cell Niches of the Subventricular Zone. Stem Cells *33*, 2232–2242.

Cahoy, J.D., Emery, B., Kaushal, A., Foo, L.C., Zamanian, J.L., Christopherson, K.S., Xing, Y., Lubischer, J.L., Krieg, P.A., Krupenko, S.A., et al. (2008). A Transcriptome Database for Astrocytes , Neurons , and Oligodendrocytes : A New Resource for Understanding Brain Development and Function. J. Neurosci. *28*, 264–278.

Fernández, M.E., Croce, S., Boutin, C., Cremer, H., and Raineteau, O. (2011). Targeted electroporation of defined lateral ventricular walls: a novel and rapid method to study fate specification during postnatal forebrain neurogenesis. Neural Dev. *6*, 13.

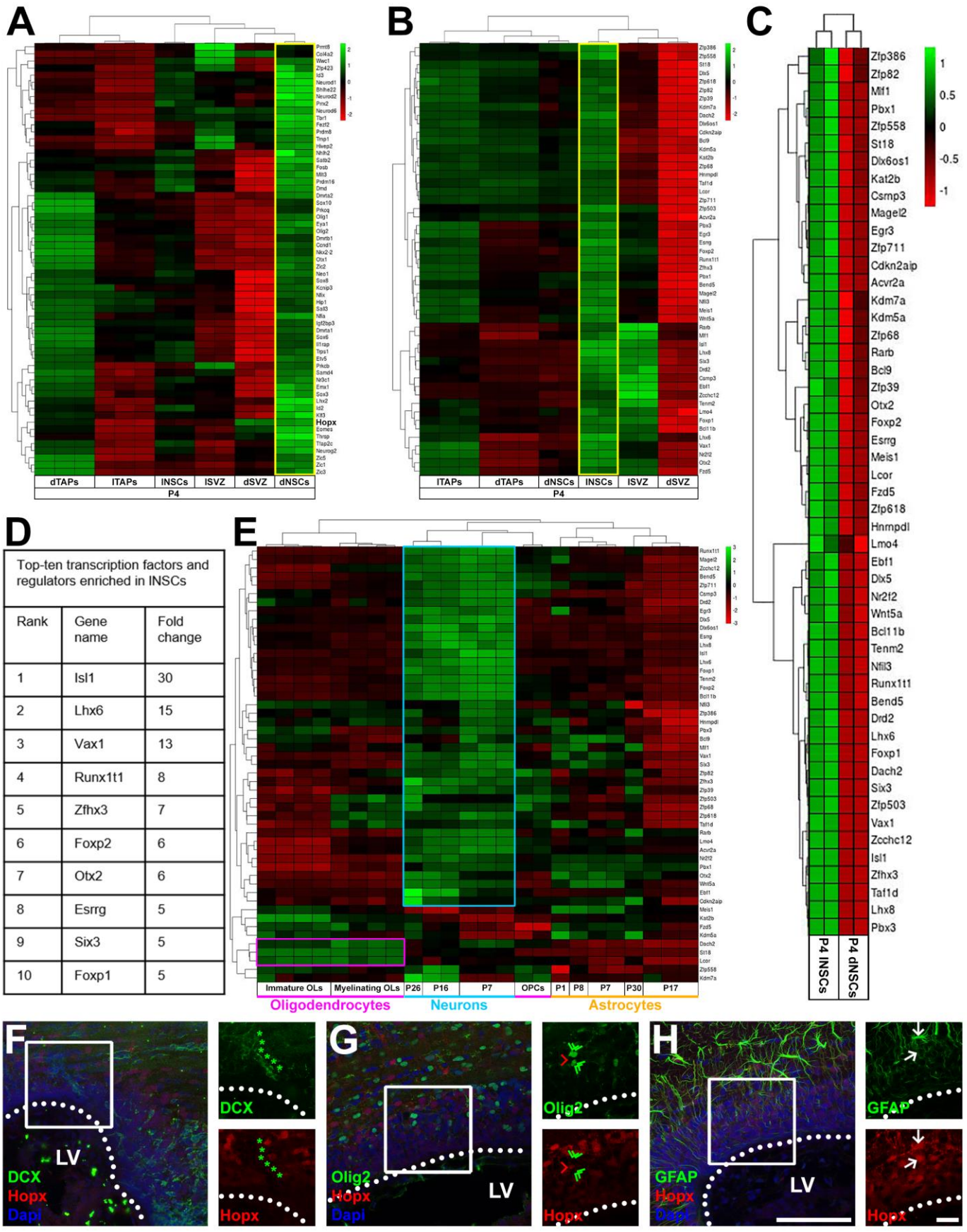

Rank	Gene name	Fold change
1	Isl1	30
2	Lhx6	15
3	Vax1	13
4	Runx1t1	8
5	Zfhx3	7
6	Foxp2	6
7	Otx2	6
8	Esrrg	5
9	Six3	5
10	Foxp1	5

Figure S1. Analysis of TFs enriched in regionally separated NSC population. Related to Figure 1

(A, B): Heatmaps confirming the enrichment of selected TF transcripts in dNSC (vs. lNSCs; A) and lNSCs (vs. dNSCs; B), including the transcriptional profile in TAPs and the environment (SVZ) of those two regions. **(C):** Heatmap of in P4 lNSCs enriched TFs compared to their dorsal counterparts (≥1,8 folds and p-value<0,05).

(D): List of the top ten TFs enriched in lNSCs.

(E): Lineage-specific meta-analysis of lNSC TFs using the dataset from the Barres group: oligodendrocytes (purple, 3/51); astrocytes (yellow, 0/51); neurons (turquoise, 42/51).

(F-H): Confirmation of astroglial lineage-specific enrichment of Hopx by immunohistochemistry within the SVZ. Hopx is absent from neuroblasts (DCX, F) and OPCs (Olig2, G), but is observed in astrocytes (GFAP, H).

Scale bars: H (overview) = 100 µm; H (crops) = 25 µm.

Abbreviations: dTAPs, dorsal transient amplifying progenitors; lTAPs, lateral transient amplifying progenitors; dNSCs, dorsal NSCs; lNSCs, lateral NSCs; dSVZ, dorsal SVZ; lSVZ, lateral SVZ; oligodendrocyte precursor cells, OPCs; OL, oligodendrocyte; LV, lateral ventricle.

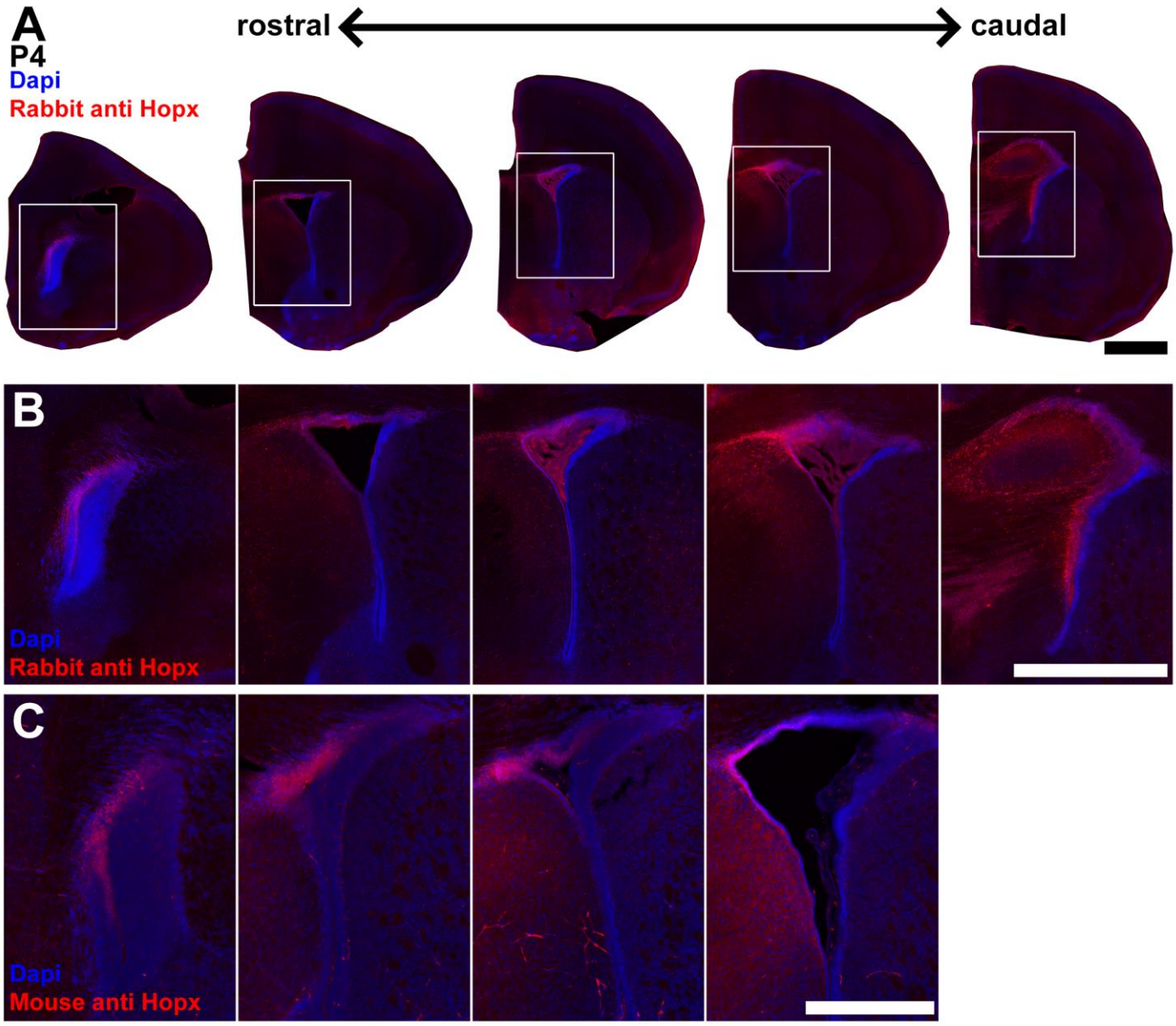

Figure S2. Spatial heterogeneity of Hopx expression at P4. Related to Figure 2

(A-C): Representative pictures demonstrate Hopx expression in a P4 animal along the rostro-caudal axis. The top and middle panel show overviews (A) and higher magnification pictures (B) of tissue stained with the rabbit anti Hopx antibody. The bottom panel shows higher magnification pictures of tissue stained with the mouse anti Hopx antibody (C). Note that both antibodies exhibit the same spatial pattern of Hopx expression. Scale bars: A, B = 1 mm; C = 500 µm.

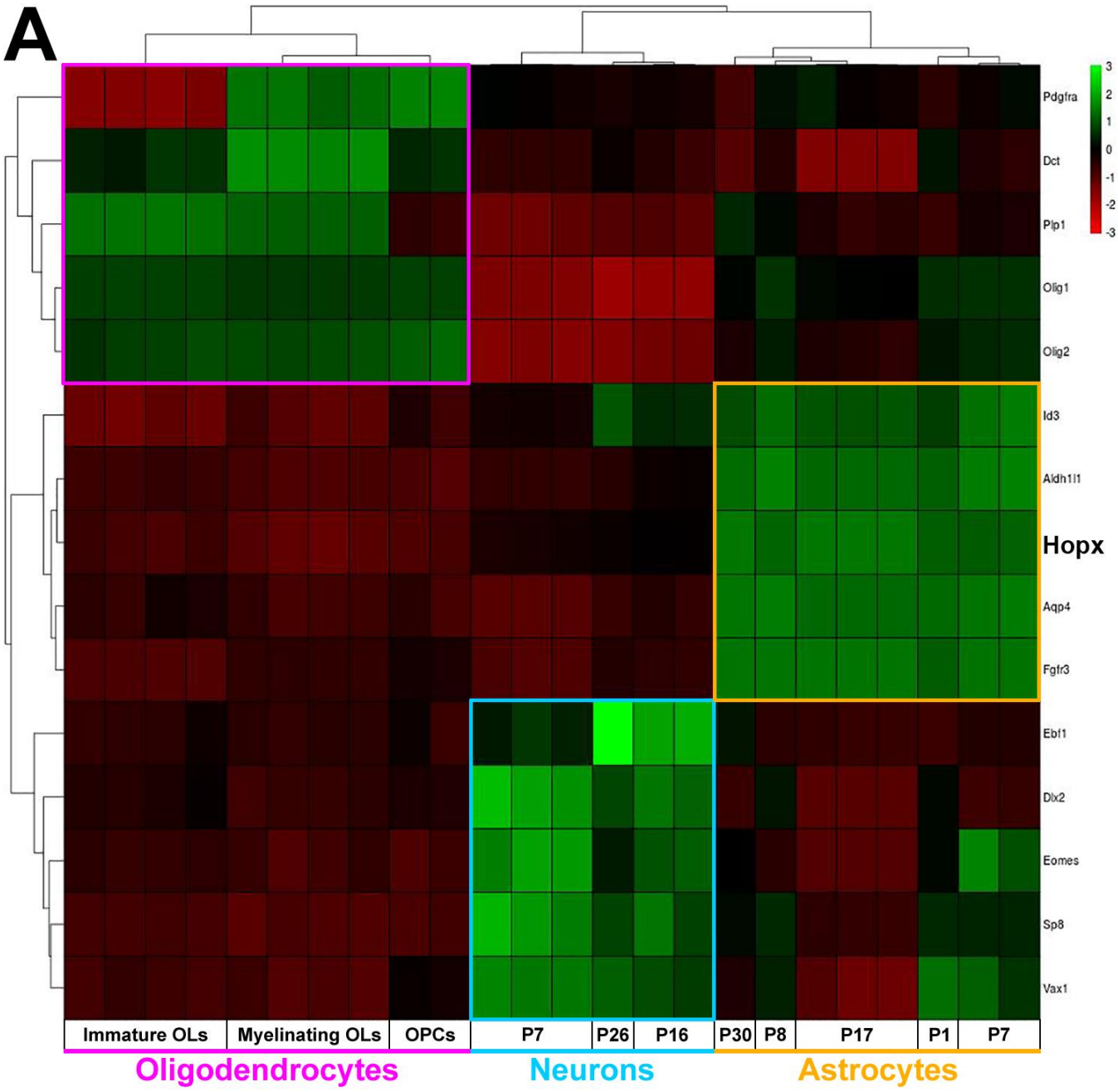

Figure S3. Confirmation of lineage specificity of selected transcripts using the dataset from the Barres group. Related to Figure 3

5 transcripts of the oligodendrocytic lineage (*PDGFRa, Dct*, *Plp1, Olig1, Olig2*), 5 of the neuronal lineage (*Ebf1, Dlx2, Eomes, Sp8, Vax1*) and 5 of the astrocytic lineage (*Id3, Aldh1l1, Hopx, Aqp4, Fgfr3*) were selected.

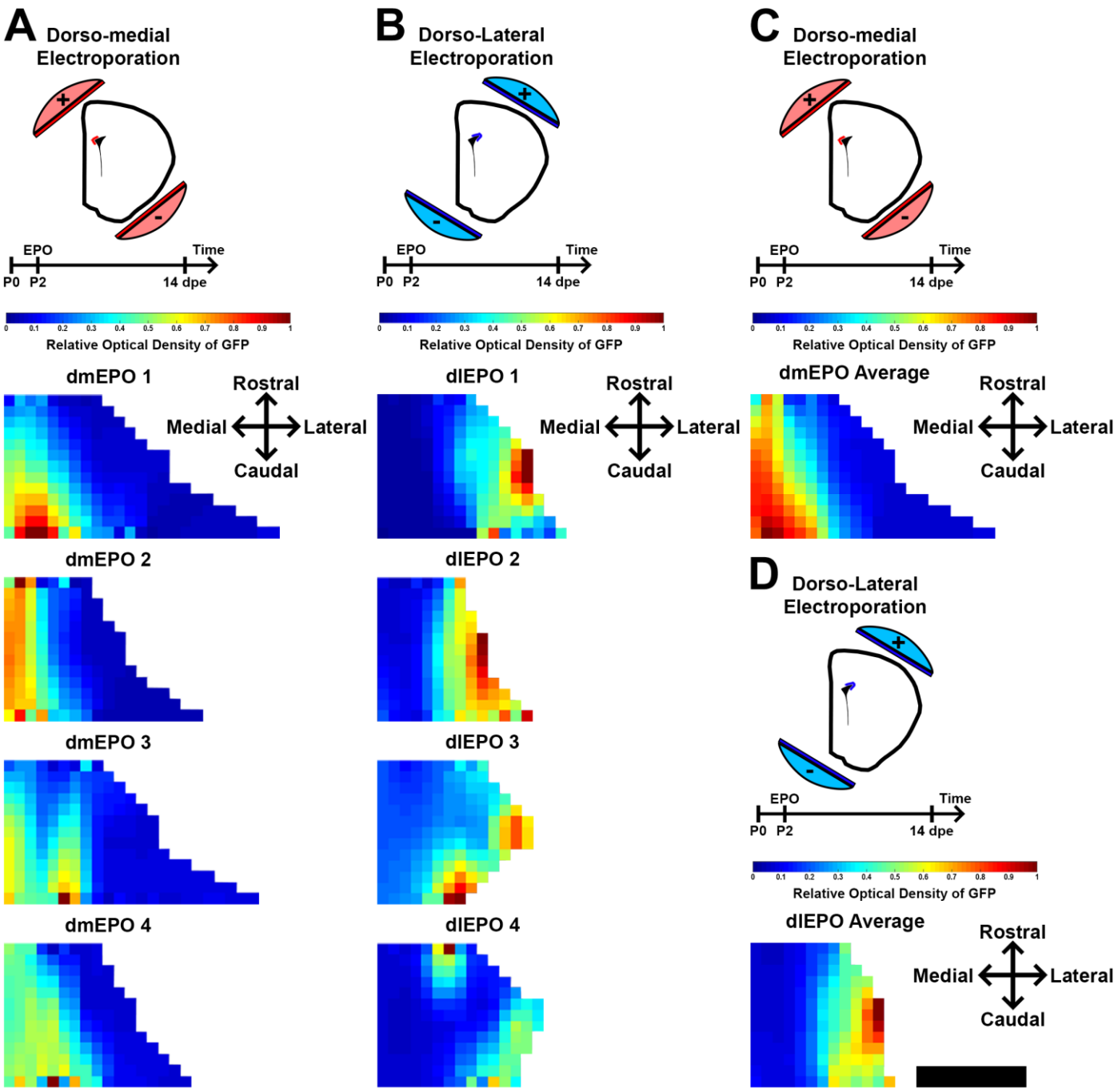

Figure S4. Optical density measurements of GFP reveal the high efficiency of targeted dorso-medial and dorso-lateral EPO. Related to Figure 3

(A+B): Heatmaps representing the relative optical density of GFP expression in the dorsal SVZ of different individuals following dorso-medial (A) or dorso-lateral EPO (14 dpe; B). Heatmaps are color coded (0 = dark blue; highest measured value = dark red). Heatmap orientation is: left = rostral; right = caudal; top = medial; bottom = lateral.

(C+D): Heatmaps representing the averaged values of 4 animals those received dorso-medial (C) or dorso-lateral EPO (D).

Animals: dmEPO, n=4; dlEPO, n=4.

Scale bar: D = 500 µm

Abbreviations: dpe, days post electroporation; EPO, electroporation; dmEPO, dorso-medial electroporation; dlEPO, dorso-lateral electroporation; SVZ, subventricular zone.

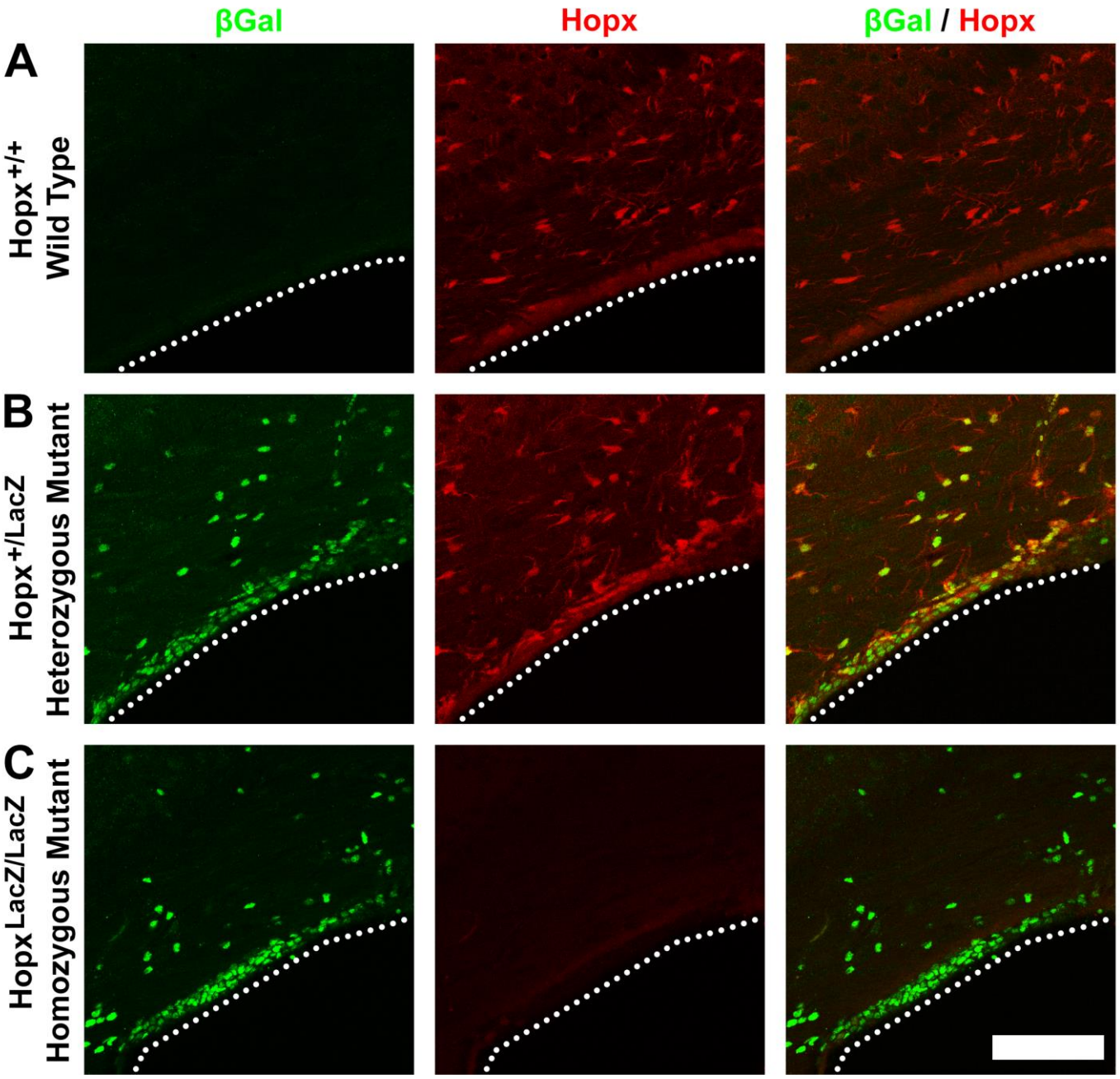

Figure S5. The Hopx$^{LacZ/WT}$ knockin transgenic mouse line. Related to Figure 5

(A-C): Co-stainings of βGal and Hopx were performed in Hopx$^{WT/WT}$ (A), Hopx$^{WT/LacZ}$ (B) and Hopx$^{LacZ/LacZ}$ (C) animals. Representative micrographs confirm the absence of βGal in Hopx$^{WT/WT}$ (A) and Hopx in Hopx$^{LacZ/LacZ}$ (C) animals, while Hopx$^{WT/LacZ}$ animals co-express both genes in the dSVZ, as well as CC (B).

Scale bar: 100 µm.

Abbreviations: βGal, β-galactosidase; dSVZ, dorsal SVZ; CC, corpus callosum; WT, wild type.

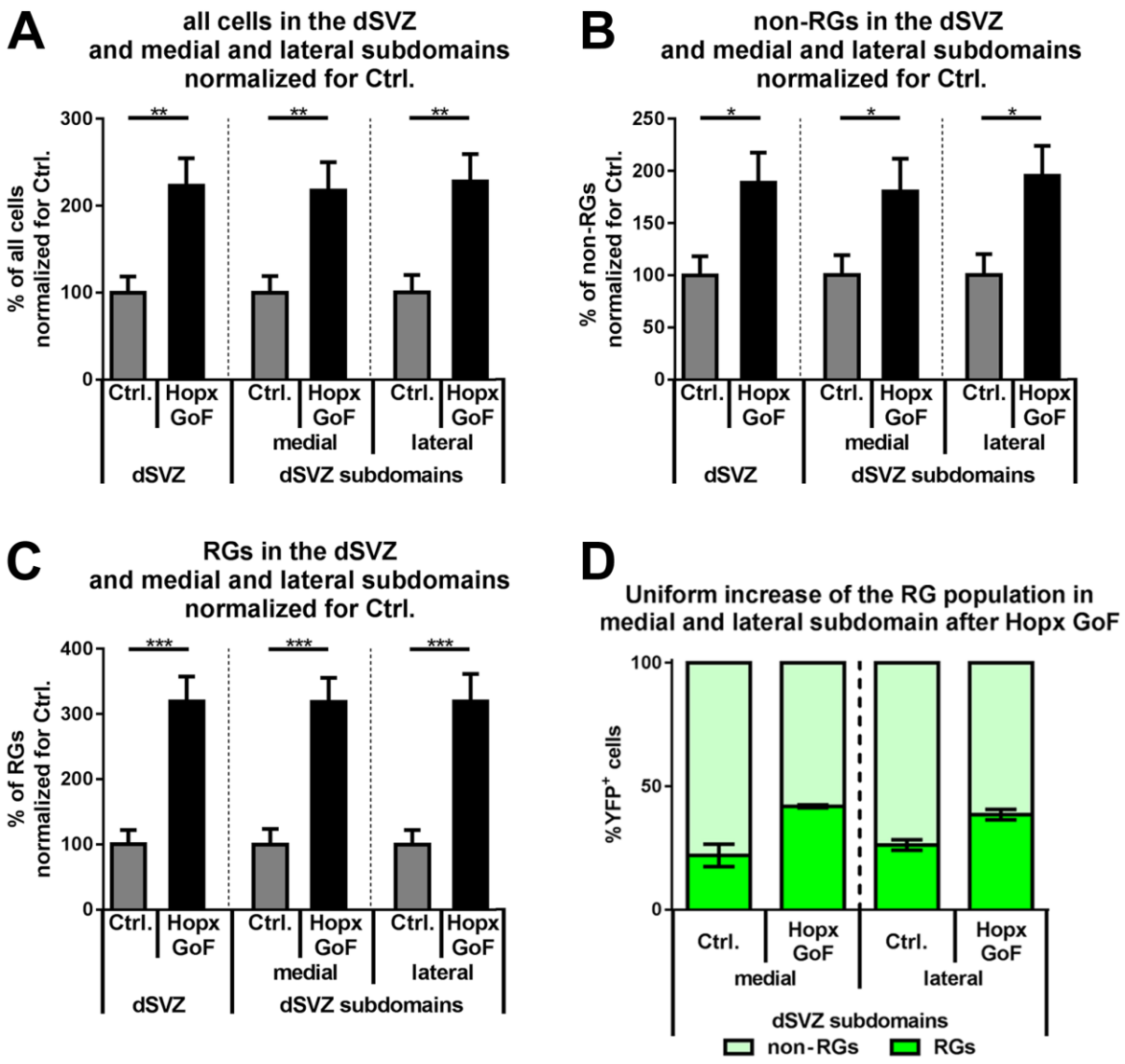

Figure S6. No difference in enlargement of the population after Hopx overexpression along the dSVZ. Related to Figure 6

(A-C): Full population (A), non-RG cells (B) and RG (C) are increased 4 days following Hopx overexpression. No difference in the enlargement between the medial and the lateral subdomain of the dSVZ was observed. Graphs are presented in percentage of the change normalized for control.

(D): The fractions of the RG population were equally increased in the medial and the lateral subdomain of the dSVZ following Hopx GoF.

Animals: Ctrl., n=7; GoF, n=5.

Abbreviations: Ctrl., control; dSVZ, dorsal SVZ; GoF, gain of function; RG, radial glia.